



# Experimental Assessment of the Flow Recirculation Effect on the Noise Measurement of a Free-Flying Multi-rotor UAS in a Closed Anechoic Chamber

Zhida Ma<sup>1</sup> · Peng Zhou<sup>1</sup> · Xin Zhang<sup>1</sup> · Siyang Zhong<sup>2</sup>

Received: 5 February 2024 / Accepted: 20 May 2024 / Published online: 12 June 2024  
© The Author(s) 2024

## Abstract

The flow recirculation effect on the noise measurement of a multi-rotor unmanned aircraft system (UAS) hovering in a closed anechoic chamber is experimentally characterized in this work. The measured acoustic spectrogram reveals that the recirculation forms around 30 s after the UAS's take-off, manifested as prominent fluctuations in blade passage frequency and its harmonics. However, the instantaneous overall sound pressure level shows no obvious increase with the development of the recirculation. The result indicates that the recirculation effect does not significantly change the total acoustic energy but increases the uncertainties in the spectral distribution, which can be quantified by spectral entropy. The quantitative analysis of different noise components shows that the recirculation has a minimal effect on the tonal noise levels but slightly increases the broadband noise level out of the rotors' plane. The results from parametric tests suggest that this broadband noise increment has a positive correlation with the UAS's hover height but a negative correlation with the UAS's gross mass. The comparison with existing studies highlights the difference in the recirculation effect on the noise of isolated rotor(s) and free-flying multi-rotor UAS in confined spaces.

**Keywords** Drone noise · Rotor noise · UAV · UAS · Turbulence ingestion · Recirculation

## 1 Introduction

With the anticipated future operation of multi-rotor unmanned aircraft system (UAS) in densely populated urban areas for various applications, the issue of their noise emissions is one of the major factors affecting public acceptance [1]. The growing public attention surrounding UAS noise necessitates the implementation of certification and regulations to mitigate this potential risk to public health [2]. The certification process requires accurate noise assessment of the UAS. Anechoic chambers provide controlled low-noise anechoic environments for accurate noise measurements and are widely used in aerospace and acoustic research. Such facili-

ties have been extensively utilized for studying the acoustic characteristics of multi-rotor UASs and their propulsion units in a controlled and echo-free setting, enabling detailed analysis of their noise generation mechanisms [3–5]. Recently, the International Organization for Standardization (ISO) published a standard on the noise measurements for UAS [6]. The standard specifies the procedures and requirements for noise measurements of UAS using anechoic chambers. However, due to the confined space, the presence of flow recirculation within anechoic chambers can introduce additional complexities to the noise measurements [7]. Since the rotors propel the fluid to produce thrust, the turbulent wake from the rotors can recirculate within the space and finally be ingested by the rotors. The ingestion of this turbulent flow leads to additional unsteady loading on the rotors' blades, which can significantly alter the aerodynamic and aeroacoustic characteristics of the rotors from them being operated in a clean inflow condition [8]. Therefore, investigations into this flow recirculation effect are important for a better understanding of the UAS noise measurements using anechoic chambers.

Previous research has been done to investigate the recirculation effect on isolated rotors. Stephenson et al. [7] tested the

✉ Siyang Zhong  
siyang.zhong@polyu.edu.hk

<sup>1</sup> Department of Mechanical and Aerospace Engineering, The Hong Kong University of Science and Technology, Clear Water Bay, Kowloon 999077, Hong Kong SAR, China

<sup>2</sup> Department of Aeronautical and Aviation Engineering, The Hong Kong Polytechnic University, Hong Hom, Kowloon 999077, Hong Kong SAR, China

noise of a small-scale propeller with a diameter  $D = 240$  mm operating at 5200 RPM in a closed anechoic chamber. The results suggest that recirculation can increase the measured noise by over 15 dB at the blade passage frequency (BPF) harmonics. They attributed this phenomenon to the unsteady loading caused by the recirculation, as the increase occurs predominantly out of the rotor plane. With the rotor producing a 0.75 lb (3.34 N) thrust, the formation time of the recirculation is around 4 s. Subsequently, with the same experimental setup, Weitsman et al. [9] studied the effect of recirculation on the force and torque measurement, as well as several treatments to mitigate the intensity of recirculation. They found that as the recirculation manifests, apart from the evident amplification in BPF harmonics, the broadband noise is also amplified. Meanwhile, the envelope of the measured thrust is modulated, and the rotational rate of the rotor presents higher fluctuation levels. The downstream mesh was found to effectively prolong the onset and reduce the intensity of the recirculation. Nadari et al. [10] performed numerical simulations and found that the flow recirculation leads to a nearly 5 dBA increase in the overall sound pressure level (OASPL) contributed by the increased SPL at BPF harmonics. Their beamforming-based source identification results suggest that the dominant mechanism for excessive noise is the leading-edge interaction at around 80% of the blade span, which is effective in the low-to-middle frequency range. A slight enhancement in the high-frequency range due to the trailing-edge noise mechanism is also identified. Bu et al. [11] measured the noise of dual small-scale ( $D = 280$  mm) rotors operating in a co-planar configuration in an anechoic chamber. At a rotational speed of 5400 RPM, the comparison with a single rotor case shows that the dual propeller configuration shortens the formation time of the recirculation from 4.5 to 2.5 s.

While stationary-mounted rotors offer more control authority and fewer uncertainties in the anechoic chamber tests, the results may not directly reflect the recirculation effect on actual multi-rotor UASs operated in such confined spaces. The presence of an airframe and the acoustic interference of different rotors can alter the noise features of a multi-rotor UAS from isolated rotors. Moreover, as no mounting structure is attached to a free-flying UAS and the rotors are not controlled at constant speeds, the system can have more degrees of freedom. Therefore, investigating the recirculation effect on the noise testing of multi-rotor UASs within confined spaces is necessary, which is the aim of this study. We conducted experimental campaigns to capture the changes in noise characteristics resulting from flow recirculation, with systematic quantitative analysis to enhance our understanding of the underlying mechanisms and their implications for noise assessment.

The following sections are arranged as follows: Sect. 2 first illustrates the experimental setup and the test procedures

to capture the formation of the recirculation. Then, the test matrix for the parametric studies on the influences of hover height and UAS mass is listed. Section 3 presents the characterization of the recirculation effect on noise, including the time-frequency spectrogram features and the quantitative analysis of sound pressure levels (SPL) of different noise components. Then, the effects of the two influencing factors are analyzed and the possible mechanisms are discussed. Section 4 summarizes the work.

## 2 Experimental Setup and Methods

### 2.1 Test Apparatus

The experiments were conducted in the anechoic chamber of the Aerodynamic and Acoustic Facility at the Hong Kong University of Science and Technology. The chamber has wedge tip-to-tip dimensions of 8.1 m (L)  $\times$  6 m (W)  $\times$  5.1 m (H) and a cut-off frequency of 100 Hz. Figure 1 shows a photo of the experimental setup.

A DJI Phantom 4 Pro quad-rotor UAS was used in the experiment. The UAS is lifted by four fixed-pitch, two-bladed, type 9450 rotors with a diameter of 240 mm. The diagonal rotor distance is 350 mm and the gross mass is 1.4 kg. During the tests, the position of the UAS was remotely controlled by a pilot outside the chamber and maintained by the visual sensing module equipped by the UAS. The onboard camera transmits real-time images to the remote control terminal and serves as a reference for the UAS to hover above the center mark. The UAS's height is estimated from its multi-sensor fused data and indicated on the remote control terminal.

The noise was measured using five 1/4" GRAS 46BE free-field condenser microphones, which were individually calibrated using a GRAS 42AG sound calibrator. The microphones were in a vertical plane that passes the horizontal center of the chamber. All microphones were equipped with windscreens to alleviate the influence of airflow on measured noise. The detailed dimensions of the microphone setup are illustrated in Fig. 1. A National Instruments PXIe-4497 module with a PXIe-1073 chassis was used to record the acoustic data. The sampling rate was 50 kHz, and a record time of 60 s was used for each test.

### 2.2 Test Methods

To capture the formation process of flow recirculation and its effect on noise measurements, a test protocol was determined. The procedures are illustrated as follows:

*Step 1* Recording starts; meanwhile, the rotors of the UAS rotate at an idle speed.

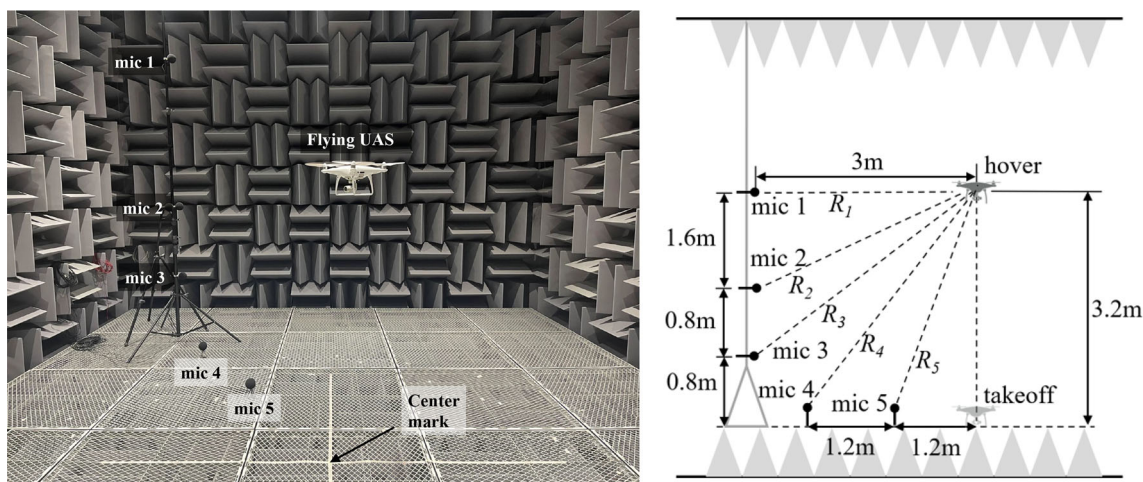


**Fig. 1** Left: photo of the experimental setup in the anechoic chamber. Right: detailed dimensions of the microphone setup with a 3.2 m UAS hover height (view perpendicular to the microphone plane)

*Step 2* Control the UAS to climb to the target hover position quickly (duration < 3 s).

*Step 3* Maintain hovering at the target position until the 60-s sampling period is over.

*Step 4* Land the UAS.

*Step 5* Wait for at least 5 min to ensure an environment with quiescent air before the next test.

Two factors that can influence the flow recirculation are investigated in this work. One is the hover height of the UAS, as it determines the recirculation flow pattern in the chamber and the turbulence intensity at the rotors' positions. The other one is the gross mass of the UAS, which determines the rotor speeds and mass flow rate through the rotor disks, consequently affecting the recirculation flow speed and overall turbulence intensity. The test matrix for the parametric investigation on these two factors is shown by Table 1. Three test data points were designed for both parameters, and four repeated tests were conducted for each data point. The heading angle of the UAS was varied such that its front, left, back, and right directions were aligned with the microphone plane in the four repeated tests, respectively.

### 2.3 Acoustic Data Post-processing

The short-time Fourier transform (STFT) is applied to the raw acoustic data to obtain the time-frequency noise characteristics, alongside Welch's method is used for smoother spectra [12, 13]. The STFT calculation uses a fast Fourier transform (FFT) size of  $10^4$  and a Hann window with 50% overlap, resulting in a frequency resolution of 5 Hz and a time resolution of 0.1 s. For the time-averaged acoustic spectra, a selected data segment is processed using an FFT size of  $10^4$  and a Hann window with 50% overlap. Figure 2 shows a

representative SPL spectrum obtained from microphone #3 when the UAS hovered at a height of 2.7 m.

To extract the tonal and broadband noise components for quantitative analyses, different techniques are applied to the raw spectrum. For the broadband noise, a moving median filter is applied to the raw spectrum to filter out the tonal spikes [14]. However, due to the wide tonal spikes caused by the fluctuations in rotor speeds, the filtered result is biased toward a higher level. Thus, a moving minimum filter is applied to the raw spectrum to account for this bias effect, and the result is averaged with the moving median spectrum. Finally, the averaged spectrum is smoothed by a Gaussian filter, which results in the desired broadband noise spectrum, as shown by the dark dashed line in Fig. 2. Considering the wide tonal spikes, tonal SPL is calculated by narrow-band integration. The band of a specific tone is defined as the part with SPL no lower than  $-20$  dB of the peak value, as shown in the right part of Fig. 2.

## 3 Results and Discussions

### 3.1 Characterization of the Recirculation Effect

Since the effect of recirculation on noise measurement of UASs can vary a lot depending on the specific test setup, a characterization of the recirculation effect is crucial before any quantitative analysis. A representative SPL spectrogram is shown in the Fig. 3. From the spectrogram, it can be observed that before the moment  $a$  ( $\sim 5$  s), the BPF shows a trend of increase–decrease–increase and then becomes constant, which corresponds to the UAS's acceleration–deceleration and hover motion. From the moment  $a$ , the tones on the spectrogram have almost no drift, indicating the UAS

**Table 1** Test matrix for the parametric investigation on the influences of hover height and gross mass

Influence factor (variable)	Hover height (m)	Gross mass (kg)
Hover height	2.2	1.4
	2.7	
	3.2	
Gross mass	2.7	1.6
		1.8
		2.0

The UAS itself weighs 1.4 kg, payloads were added to vary the gross mass

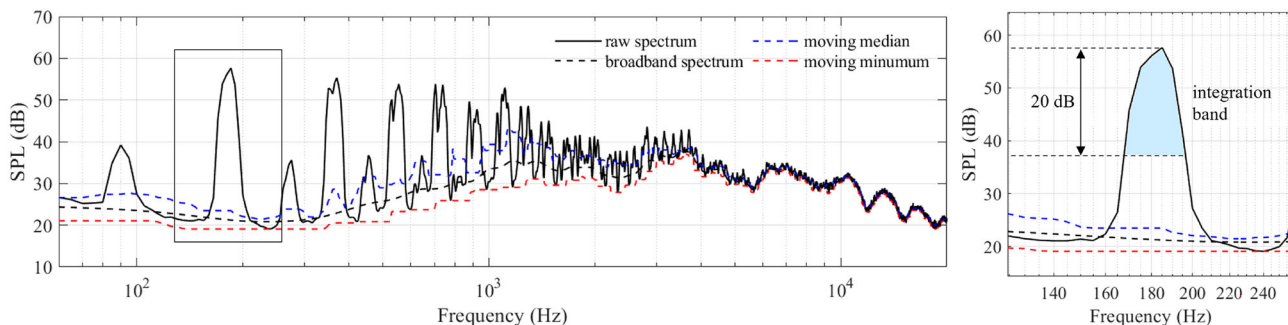


**Fig. 2** Left: raw spectrum, spectra processed using moving median and moving minimum algorithms, respectively, and the resultant broadband spectrum of a test case. Right: zoomed view at the SPL spike at BPF, the band of this tone is defined as the part with SPL no lower than  $-20$  dB of the peak level, and the tonal SPL is calculated by the spectral integration within this band

entered a relatively stable hover condition. At around the moment  $b$  ( $\sim 30$  s), prominent random fluctuations of BPF harmonics arise on the spectrogram as a result of the unstable rotor speeds. This is inferred to be caused by the recirculation of the rotors’ wake, which leads to the turbulent inflow of the rotors and disturbances to the stable hover state. The fluctuations in BPF harmonics are a consequence of the UAS trying to maintain its position under these disturbances. Therefore, the moment  $b$  can be regarded as the transition from a pre-recirculation flow regime to a post-recirculation regime. It is worth noting that the precise determination of this transition moment is not feasible as the intensity of the tonal fluctuations increases gradually.

Although obvious fluctuations can be observed on the spectrogram, the instantaneous OASPL integrated from 100 to 20,000 Hz, as shown by the blue curve in Fig. 3, does not show a significant deviation after the recirculation develops but presents slight higher fluctuation values up to 2 dB. Hence, the instantaneous OASPL value cannot distinguish the transition into the post-recirculation flow regime. To quantify these uncertain fluctuations that appear on the spectrogram, spectral entropy (SE), a spectral descriptor reflecting the irregularity of the signal in the frequency domain, is introduced [15]. For a given power spectrogram  $S(t, k)$ , the frequency domain probability distribution within a certain frequency band at time  $t$  is:

$$P(t, k) = \frac{S(t, k)}{\sum_{k=b_1}^{b_2} S(t, k)}, \tag{1}$$

where  $k$  represents the frequency bin number,  $b_1$  and  $b_2$  are the frequency band edges in bins. The instantaneous SE within this band is calculated as [16]:

$$SE(t) = \frac{-\sum_{k=b_1}^{b_2} P(t, k) \log(P(t, k))}{\log(b_2 - b_1)}. \tag{2}$$

Since the fluctuations of BPF harmonics occur in a relatively low-frequency range, the frequency band of 100 Hz to 2000 Hz is chosen for SE calculations herein. An FFT size of  $10^5$  and a Hann window with 50% overlap are used to match the timescale of the spectral fluctuations. The result of the test case is shown by the orange curve in Fig. 3. It can be seen that from the moment  $a$ , following a dramatic drop after the take-off maneuver, the SE stays at a relatively low value. Around the moment  $b$ , which is in the transition region, the SE gradually increases by about 0.1 (17%) and remains at a relatively high value afterward. The SE exhibits a consistent trend with the fluctuation intensity of the tonal frequencies in the spectrogram and, therefore, can be used as a reference to detect the formation of the recirculation.

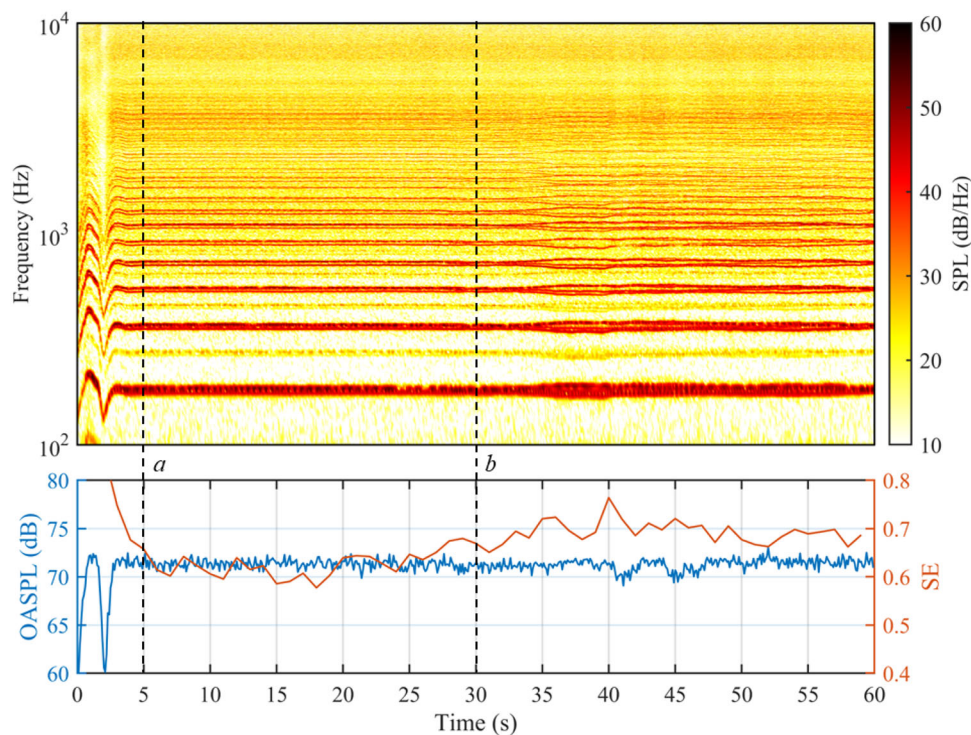


**Fig. 3** Top: the measured spectrogram at microphone #3 with a hover height of 3 m and UAS gross mass of 1.4 kg. Bottom: instantaneous OASPL and SE values

The detailed SPL spectral difference between the pre- and post-recirculation regimes in the aforementioned test case is shown in Fig. 4. The SPL spectra are computed using 20-s segments from the total 60-s data for the two flow regimes. The segment for the pre-recirculation regime is from 5 to 25 s, while the segment for the post-recirculation regime is from 35 to 55 s. It is evident that in the post-recirculation regime, the tonal spikes become broader, and two or more separated spikes can be present at high-order BPF harmonics. Meanwhile, the peak values of the tonal spikes generally decrease following the formation of the recirculation, and the decrements are more prominent at higher BPF harmonics. This phenomenon is attributed to the time-averaged impact of rotor speed fluctuations caused by recirculation disturbances.

Notably, the results of this experiment diverge from those reported by the existing experimental studies, in which cases substantial increases in SPL were measured at blade-passing frequency (BPF) harmonics due to flow recirculation [7, 9, 11]. Several factors are speculated to account for the disparity. First, the chamber used in our work is significantly larger, approximately 8 and 12 times the volume of the ones employed by Stephenson et al. [7] and Bu et al. [11], respectively. This disparity results in lower turbulence intensity within the recirculation zone and a longer onset time. Sec-

ond, the rotor-airframe interaction in our case is expected to generate high SPLs at BPF harmonics, which can potentially outweigh the effect of flow recirculation [17, 18]. This interaction mechanism is unlikely to be dominant in other studies as there are no structures in proximity to the rotor blades. Last but not least, with more degrees of freedom, the hovering UAS's rotors in our case experience greater speed fluctuations compared to a statically mounted single rotor, causing the acoustic energy to disperse around BPF harmonics rather than being concentrated at specific frequencies.

A quantitative comparison of the tonal SPL of the first four BPF harmonics and broadband OASPL, as well as SE between the pre- and post-recirculation flow regimes from the test case are presented in Table 2. The SPL data are processed using the method outlined in Sect. 2.3. The results indicate that the tonal noise levels remain largely unaffected by the presence of flow recirculation. Meanwhile, a slight increase in the extracted broadband noise level is observed particularly out of the UAS's rotor plane. This increment is inferred to be caused by the enhanced unsteady blade loading due to the ingestion of the recirculated turbulent structures, and the directivity trend is consistent with the characteristics of loading noise [19]. The SE increases by 0.07~0.08 (12%~13%) at tested microphone locations, no prominent directivity was found for the SE increments.

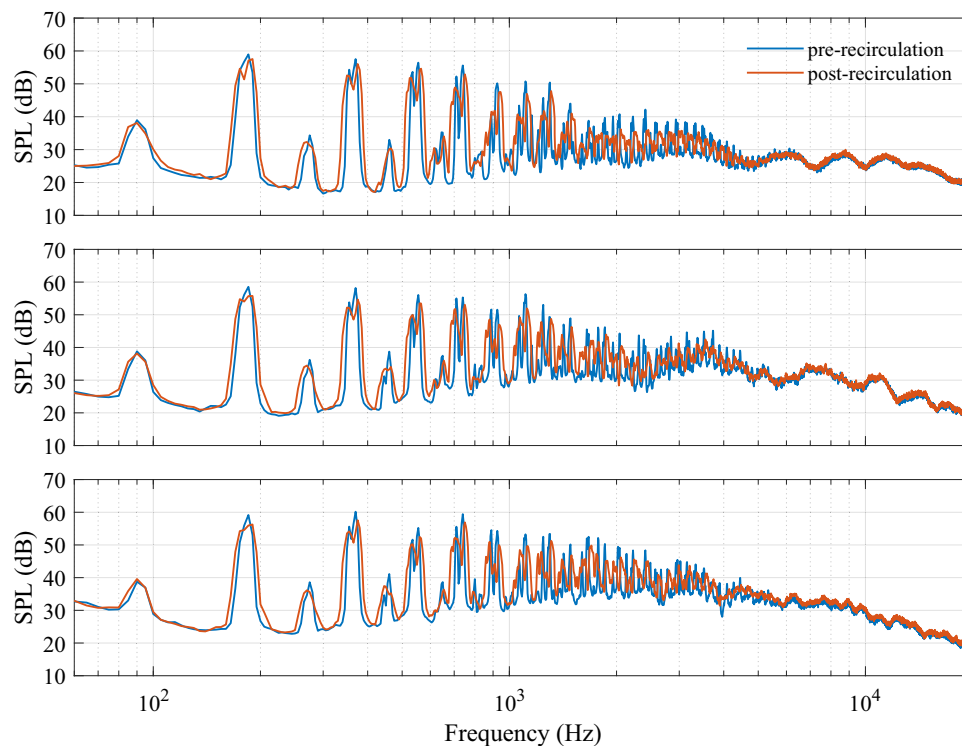


**Fig. 4** Comparison of the SPL spectra measured in pre- and post-recirculation flow regimes at microphones #1 (top), #3 (middle), and #5 (bottom)

**Table 2** SPL variations of different noise components and SE variation between pre- and post-recirculation flow regimes

Microphone	$\Delta\text{SPL}_{1\text{BPF}}$ (dB)	$\Delta\text{SPL}_{2\text{BPF}}$ (dB)	$\Delta\text{SPL}_{3\text{BPF}}$ (dB)	$\Delta\text{SPL}_{4\text{BPF}}$ (dB)	$\Delta\text{OASPL}_{\text{broadband}}$ (dB)	$\Delta\text{SE}$
#1	−0.25	0.25	0.21	−0.54	1.08	0.068
#2	−0.24	−0.84	0.66	−0.27	1.26	0.073
#3	−0.16	−0.89	0.40	−0.24	1.43	0.083
#4	−0.15	−0.69	0.39	−0.12	1.29	0.079
#5	−0.13	−0.53	0.04	0.02	2.03	0.082

$$\Delta\text{SPL} = \text{SPL}_{\text{post-recirculation}} - \text{SPL}_{\text{pre-recirculation}}, \Delta\text{SE} = \text{SE}_{\text{post-recirculation}} - \text{SE}_{\text{pre-recirculation}}$$

### 3.2 Effect of Hover Height

The results for the parametric study on the effect of hover height are shown in Fig. 5. Significantly higher standard variations of the 1BPF tonal SPL when the UAS was hovering at 2.7 m are present on the graph. After a data examination, this is caused by the data from a single test and can be attributed to testing uncertainty. The general SPL differences between the two flow regimes are consistent with the aforementioned test case, which is almost no variations in the tonal SPL, and slight increases in the broadband OASPLs. The variation in hover height does not have a prominent effect on the tonal SPL differences, but the broadband OASPL increment has a discernible increasing trend with the hover height. This trend suggests that the intensity of the rotors' interaction with the recirculation enhances when the UAS hovers at a higher height. Speculations for this phenomenon are that at

a higher height, the UAS is hovering closer to the ceiling, where the recirculated flow is expected to be less uniform and non-axial to the rotors, leading to stronger disturbances to the UAS and higher levels of unsteady blade loading [20]. While the UAS hovers at a lower height yet still far from encountering the aerodynamic ground effect, the inflow of the rotors becomes more aligned with the axial direction due to the induced velocity, and the turbulence intensity can be reduced after a longer convection distance.

### 3.3 Effect of Gross Mass

Figure 6 shows the SPL differences of the UAS hovering under varied payload mass. Similar to the previous cases, there are no obvious variations in tonal SPLs, but slight increases in the broadband OASPLs are observed after the recirculation develops. An interesting and counterintuitive

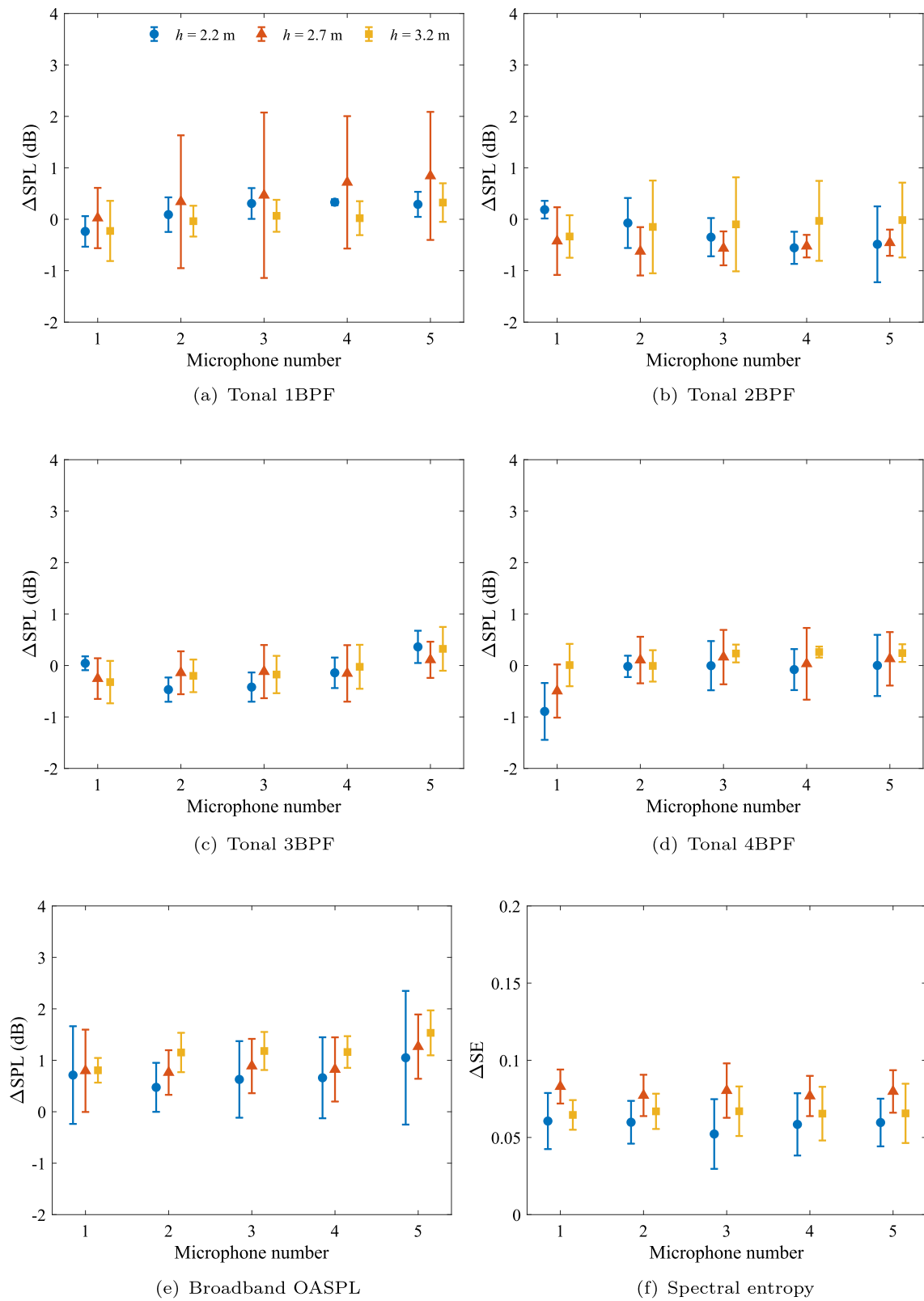


**Fig. 5** SPL variations of different noise components and SE variation between the two flow regimes. Data points are the averaged value from four repeated tests, error bars indicate the  $\pm 1$  standard deviation

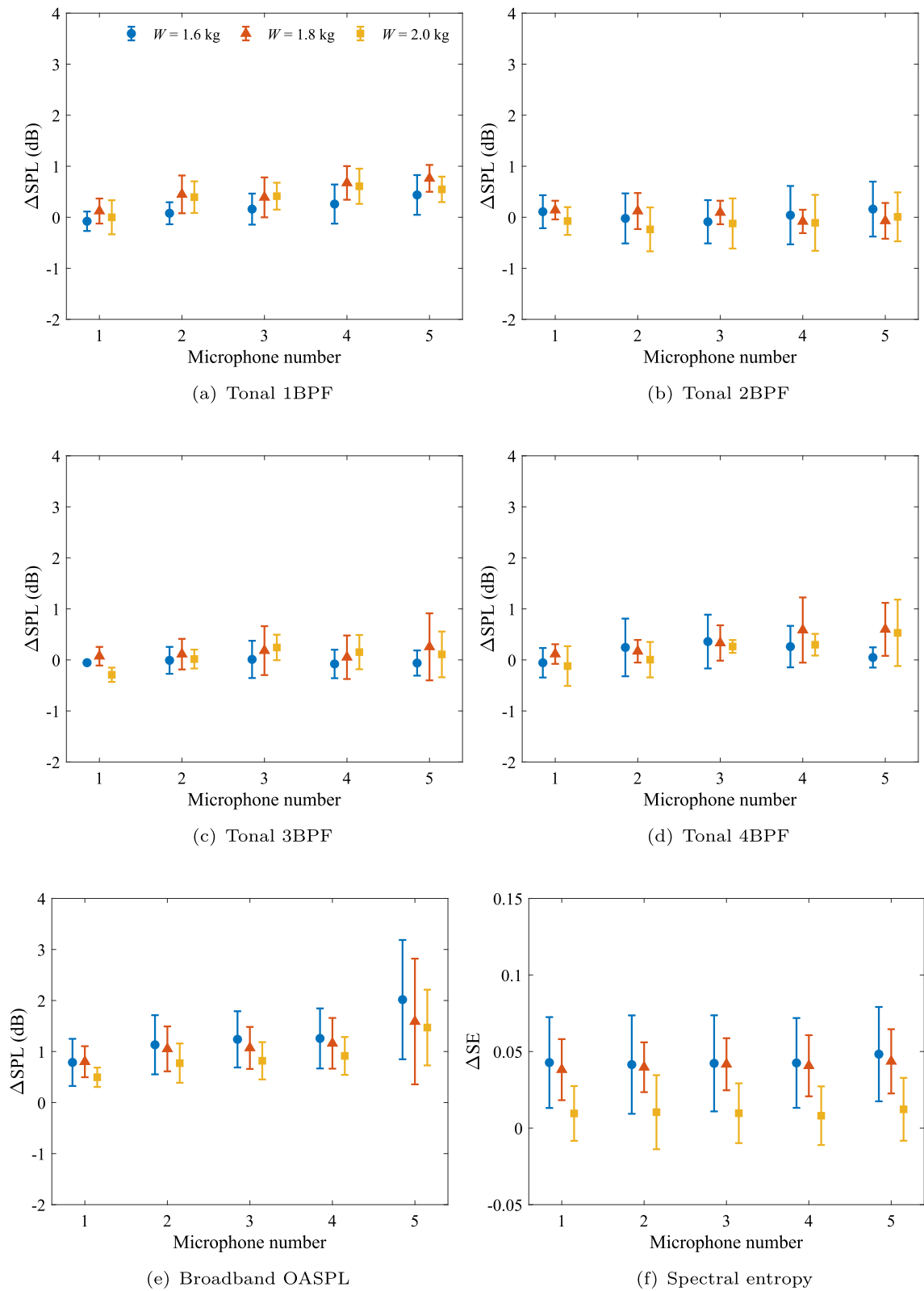


**Fig. 6** SPL variations of different noise components and SE variation between the two flow regimes. Data points are the averaged value from four repeated tests, error bars indicate the  $\pm 1$  standard deviation

result is that the broadband OASPL increment shows a decreasing trend with the gross mass. Meanwhile, the uncertainties in broadband OASPL also reduce. The reason for this phenomenon is most possibly that the increased payload mass adds inertia to the UAS, making it less vulnerable to the disturbances caused by the recirculation. This stabilizing effect can lead to fewer rotor speed fluctuations, hence reducing the enhancement of broadband noise.

## 4 Summary

The experimental results have characterized the effect of the flow recirculation on the acoustic measurement of a free-flying multi-rotor UAS in a closed anechoic facility. The major effect is the disturbances caused by the recirculated turbulent structures to the hovering UAS, leading to fluctuations in rotor speeds and, consequently, uncertainties in the tonal noise. These uncertainties lead to a more random spectral distribution of the acoustic energy, but the measured OASPL remains at the same level throughout the development of the recirculation. Spectral entropy is introduced to quantify these uncertainties in the frequency domain, and the calculated SE shows a reasonable increasing trend with the formation of the recirculation. The SPLs of different noise components extracted using the proposed method indicate that the recirculation has a negligible effect on the tonal SPLs at the first four BPF harmonics but slightly ( $\sim 2$  dB) enhances the broadband OASPL out of the rotor plane. The parametric investigation reveals that the broadband noise increment due to recirculation has a positive correlation with the hover height of the UAS but a negative correlation with the UAS's gross mass. Higher flow nonuniformity due to ceiling effect and increased inertia are inferred to be the major reasons accounting for these two correlations, respectively.

The effect of flow recirculation on measured noise in this study differs from those reported in existing studies [7, 9, 11]. Notably, a significantly lesser influence on the noise level due to recirculation is observed. Although the difference in the dimension of the test facility shall be acknowledged, the comparison highlights the distinction between testing statically mounted propulsion unit(s) and free-flying UASs in such confined environments. One aspect is the presence of an airframe and multiple rotors can lead to strong interactions, which make the noise characteristics of the UAS inherently different from those of a propulsion unit mounted on a test rig. Another aspect is that the recirculation can disturb the hover state of the UAS and lead to fluctuations in rotor speeds, which cause extra uncertainties in noise compared to rotors controlled at constant speeds. Therefore, a characterization of

the flow recirculation effect before conducting any accurate acoustic assessments is important for UAS noise assessments in closed facilities.

**Funding** Open access funding provided by The Hong Kong Polytechnic University.

**Open Access** This article is licensed under a Creative Commons Attribution 4.0 International License, which permits use, sharing, adaptation, distribution and reproduction in any medium or format, as long as you give appropriate credit to the original author(s) and the source, provide a link to the Creative Commons licence, and indicate if changes were made. The images or other third party material in this article are included in the article's Creative Commons licence, unless indicated otherwise in a credit line to the material. If material is not included in the article's Creative Commons licence and your intended use is not permitted by statutory regulation or exceeds the permitted use, you will need to obtain permission directly from the copyright holder. To view a copy of this licence, visit <http://creativecommons.org/licenses/by/4.0/>.

## References

- Schäffer, B., Pieren, R., Heutschi, K., Wunderli, J.M., Becker, S.: Drone noise emission characteristics and noise effects on humans—a systematic review. *Int. J. Environ. Res. Public Health* **18**(11), 5940 (2021)
- Torija, A.J., Nicholls, R.K.: Investigation of metrics for assessing human response to drone noise. *Int. J. Environ. Res. Public Health* **19**(6), 3152 (2022)
- Zawodny, N.S., Douglas Boyd Jr, D., Burley, C.L.: Acoustic characterization and prediction of representative, small-scale rotary-wing unmanned aircraft system components. *American Helicopter Society (AHS) Annual Forum Proceedings*, (NF1676L-22587) (2016)
- Zhou, T., Jiang, H., Sun, Y., Fattah, R.J., Zhang, X., Huang, B., Cheng, L.: Acoustic characteristics of a quad-copter under realistic flight conditions. *AIAA Paper*, 2019-2587 (2019)
- Huanxian, B., Ma, Z., Zhong, S.: An experimental investigation of noise characteristics of overlapping propellers. *J. Acoust. Soc. Am.* **152**(1), 591–600 (2022)
- International Organization for Standardization. ISO 5305:2024 Noise measurements for UAS (unmanned aircraft systems). Geneva, CH (2024)
- Stephenson, J.H., Weitsman, D., Zawodny, N.S.: Effects of flow recirculation on unmanned aircraft system (UAS) acoustic measurements in closed anechoic chambers. *J. Acoust. Soc. Am.* **145**(3), 1153–1155 (2019)
- Hanson, D.B.: Spectrum of rotor noise caused by atmospheric turbulence. *J. Acoust. Soc. Am.* **56**(1), 110–126 (1974)
- Weitsman, D., Stephenson, J.H., Zawodny, N.S.: Effects of flow recirculation on acoustic and dynamic measurements of rotary-wing systems operating in closed anechoic chambers. *J. Acoust. Soc. Am.* **148**(3), 1325–1336 (2020)
- Nardari, C., Casalino, D., Polidoro, F., Coralic, V., Lew, P-T., Brodie, J.: Numerical and experimental investigation of flow confinement effects on UAV rotor noise. *AIAA Paper*, 2019-2497 (2019)

11. Huanxian, B., Han, W., Bertin, C., Fang, Y., Zhong, S.: Aerodynamic and acoustic measurements of dual small-scale propellers. *J. Sound Vib.* **511**, 116330 (2021)
12. Fulop, S.A., Fitz, K.: Algorithms for computing the time-corrected instantaneous frequency (reassigned) spectrogram, with applications. *J. Acoust. Soc. Am.* **119**(1), 360–371 (2006)
13. Welch, P.: The use of fast fourier transform for the estimation of power spectra: a method based on time averaging over short, modified periodograms. *IEEE Trans. Audio Electroacoust.* **15**(2), 70–73 (1967)
14. Fitzgerald, D.: Harmonic/percussive separation using median filtering. In: *Proceedings of the 2010 International Conference on Digital Audio Effects (DAFx)* **13**, pp. 1–4 (2010)
15. Shannon, C.E.: A mathematical theory of communication. *Bell Syst. Techn. J.* **27**(3), 379–423 (1948)
16. Misra, H., Ikbal, S., Bourlard, H., Hermansky, H.: Spectral entropy based feature for robust ASR. In: *Proceedings of the 2004 IEEE International Conference on Acoustics, Speech, and Signal Processing (ICASSP)* **1**, pp. I–193 (2004)
17. Zawodny, N.S., Boyd, D.D.: Investigation of rotor-airframe interaction noise associated with small-scale rotary-wing unmanned aircraft systems. *J. Am. Helicopter Soc.* **65**(1), 1–17 (2020)
18. Yan, W., Kingan, M.J., Go, S.T.: Propeller-strut interaction tone noise. *Phys. Fluids* **34**(5) (2022)
19. Kurtz, D.W., Marte, J.E.: A review of aerodynamic noise from propellers, rotors, and lift fans. NASA Technical Report, NASA-32-7462 (1970)
20. Gao, S., Di Franco, C., Carter, D., Quinn, D., Bezzo, N.: Exploiting ground and ceiling effects on autonomous UAV motion planning. In: *Proceedings of the 2019 International Conference on Unmanned Aircraft Systems (ICUAS)*, pp. 768–777 (2019)

**Publisher's Note** Springer Nature remains neutral with regard to jurisdictional claims in published maps and institutional affiliations.